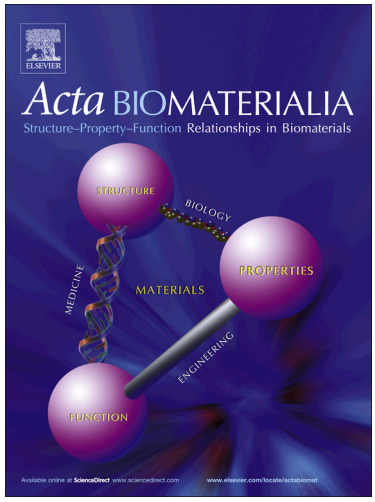

Gold-Nanoparticles coated with the antimicrobial peptide Esculentin-1a(1-21)NH_2 as a reliable strategy for antipseudomonal drugs

Bruno Casciaro, Maria Moros, Sara Rivera-Fernandez, Andrea Bellelli, Jesús M de la Fuente, Maria Luisa Mangoni

PII: S1742-7061(16)30514-1
DOI: http://dx.doi.org/10.1016/j.actbio.2016.09.041
Reference: ACTBIO 4462

To appear in: *Acta Biomaterialia*

Received Date: 6 June 2016
Revised Date: 26 September 2016
Accepted Date: 28 September 2016

Please cite this article as: Casciaro, B., Moros, M., Rivera-Fernandez, S., Bellelli, A., de la Fuente, J.M., Luisa Mangoni, M., Gold-Nanoparticles coated with the antimicrobial peptide Esculentin-1a(1-21)NH_2 as a reliable strategy for antipseudomonal drugs, *Acta Biomaterialia* (2016), doi: http://dx.doi.org/10.1016/j.actbio.2016.09.041

Gold-Nanoparticles coated with the antimicrobial peptide Esculentin-1a(1-21)NH_2 as a reliable strategy for antipseudomonal drugs

Bruno Casciaro,[a¥] Maria Moros,[b¥] Sara Rivera-Fernandez,[c] Andrea Bellelli,[a] Jesús M de la Fuente,[c*] Maria Luisa Mangoni[a*]

[¥] These authors equally contributed to the work

[a]Istituto Pasteur-Fondazione Cenci Bolognetti, Department of Biochemical Sciences, Sapienza University of Rome, Rome, Italy; [b]Istituto di Scienze Applicate e Sistemi Intelligenti, CNR, Pozzuoli, Italy; [c]Instituto de Ciencia de Materiales de Aragon-CSIC/Universidad de Zaragoza, Spain

* Correspondence to:

Maria Luisa Mangoni, Department of Biochemical Sciences, Sapienza University of Rome.

Via degli Apuli, 9-00185, Rome-Italy; Phone: +39 06 49917693.

Email: marialuisa.mangoni@uniroma1.it

and

Jesús M de la Fuente

Instituto de Ciencia de Materiales de Aragon-CSIC/Universidad de Zaragoza -Spain. Phone: +34 606949073. Email: jmfuente@unizar.es

Abstract

Naturally occurring antimicrobial peptides (AMPs) hold promise as future therapeutics against multidrug resistant microorganisms. Recently, we have discovered that a derivative of the frog skin AMP esculentin-1a, Esc(1-21), is highly potent against both free living and biofilm forms of the bacterial pathogen *Pseudomonas aeruginosa.* However, bringing AMPs into clinics requires to overcome their low stability, high toxicity and inefficient delivery to the target site at high concentrations. Importantly, peptide conjugation to gold nanoparticles (AuNPs), which are among the most applied inorganic nanocarriers in biomedical sciences, represents a valuable strategy to solve these problems. Here we report that covalent conjugation of Esc(1-21) to soluble AuNPs [AuNPs@Esc(1-21)] *via* a poly(ethylene glycol) linker increased by ~15-fold the activity of the free peptide against the motile and sessile forms of *P. aeruginosa* without being toxic to human keratinocytes. Furthermore, AuNPs@Esc(1-21) resulted to be significantly more resistant to proteolytic digestion and to disintegrate the bacterial membrane at very low concentration (5 nM). Finally, we demonstrated for the first time the capability of peptide-coated AuNPs to display a wound healing activity on a keratinocytes monolayer. Overall, these findings suggest that our engineered AuNPs can serve as attractive novel biological-derived material for topical treatment of epithelial infections and healing of the injured tissue.

Keywords: antimicrobial peptide; gold nanoparticles; *Pseudomonas aeruginosa*; membrane perturbation, anti-biofilm activity, electron microscopy; wound healing; biostability.

1. Introduction

Microbial resistance to the existing antibiotics has developed on a very large scale over time [1]. It has now turned into a serious life-threat and a significant burden to healthcare systems due to prolonged hospitalization, therapies and care costs [2]. This global problem compelled the World Health Organization to express its concerns regarding the beginning of a new pre-antibiotic era in the 21st century [2]. Hence, the discovery of new anti-infective agents with a different mode of action is in great demand [3], and naturally-occurring antimicrobial peptides (AMPs) would be up-and-coming substitutes for the generation of a new class of antibiotics [4]. AMPs occur in all kingdoms of life where they are produced as part of the innate defense mechanism against microorganisms [5, 6]. Despite differences in their sequence and secondary structure, they are characterized by a small size (10-50 amino acids) and can be classified into cationic (the majority of them) or anionic AMPs (such as maximin H5 or dermcidin [7-11]), on the basis of their net charge at neutral pH [12]. Traditionally, these peptides have been described as "antimicrobial" because of the ability to kill microorganisms by disrupting their membrane [12]. Lately, however, some of them have been found to target different sites in bacteria (i.e. ribosomes) [13, 14] and/or to display immunomodulatory features (e.g. anti-endotoxin, chemotaxis, pro-inflammatory, wound healing properties), and have been referred to more properly as "host-defense peptides" [15-17]. In particular, AMPs with an alpha helical structure exert a bactericidal activity by mainly perturbing the anionic microbial membrane, with leakage of cytosolic components [18-20]. This is in contrast with the specific mechanism of action of conventional antibiotics. They generally interfere with some crucial intracellular functions (e.g. inhibition of DNA, RNA, protein synthesis or enzymatic activity) [7], upon interaction with a single target. These targets are mainly proteins, that are highly susceptible to mutations [21, 22]. This would prevent the antibiotics from recognizing their altered target, thus making it easier for them to select for resistant microorganisms [23]. Differently, to acquire resistance to AMPs, microbes should modify the lipid composition of their membrane, but

this could not happen without provoking a lethal damage to themselves [24]. It is noteworthy that several AMPs have already entered clinical trials mostly for the development of antimicrobials for topical treatment of severe infection diseases, including those induced by multi-drug resistant Gram-negative bacteria like *Pseudomonas aeruginosa* [3, 25]. *P. aeruginosa* is an opportunistic pathogen causing a wide range of systemic or local infections, such as otitis, keratitis, pneumonia and skin (burn wounds) infections, primarily in immunocompromised patients [26]. This bacterium has a high degree of adaptability to hostile environments, a high intrinsic resistance to conventional antibiotics and propensity to adhere to both abiotic or biological surfaces forming biofilms that available drugs cannot debate [27-30]. Importantly, new efficacious antimicrobial agents (i.e. AMPs) should be able not only to eradicate both forms of growth of this microorganism but also to restore the integrity of the damaged infected tissue, e.g. by displaying wound healing properties [31, 32]. However, among major drawbacks in developing AMPs as future therapeutics; (i) the poor pharmacokinetic profile due to degradation by serum proteases and rapid clearance by renal filtration; (ii) the toxicity towards mammalian cells [33]; (iii) the scarce tissue diffusibility and (iv) the inefficient delivery to the target site, take hold. In this scenario, the usage of peptide-coated nanoparticles (NPs) represents a valuable solution to circumvent these limitations [34, 35]. Functionalized NPs, in general, have attracted the attention of the scientific community for the manufacturing, imaging, diagnosis and delivery of antibacterial drugs [36-41]. Indeed, packaging antibiotic compounds within the same NPs would enable not only to protect the drug from the external environment but also to concentrate it at the desired infection site reaching doses much higher than those achievable upon administration of free drug molecules [42, 43]. Gold NPs (AuNPs) are among the most applied inorganic nanocarriers in the field of biomedical sciences [44-46]. Among their advantages, AuNPs can be easily synthesized with a wide range of sizes and shapes, functionalized with a great variety of molecules and are considered biocompatible. Also, AuNPs exhibit an absorption band that occurs when the incident photon frequency is in resonance with the collective oscillation of the conductive band electrons, called localized surface plasmon

resonance band [47]. This band can be tuned throughout visible to near infrared wavelengths, and can be used to calculate the size and concentration of the AuNPs in solution. To date, AuNPs are being tested from immunoassay application to *in vivo* cancer targeting, specific delivery of siRNA without undesirable immune response, and/or imaging [48-50].

However to date, comprehensive studies of AuNPs on bacteria have rarely been carried out and very little is known about the biological effect(s) of AuNPs conjugated to AMPs. Amongst AMPs of natural origin, we have recently identified a derivative of the frog skin AMP esculentin-1a, Esculentin-1a(1-21)NH_2 [Esc(1-21)], GIFSKLAGKKIKNLLISGLKG-NH_2, corresponding to the first 20 residues of esculentin-1a plus a glycinamide at its C-terminus [51], with a strong activity against both free-living and sessile forms of either reference or clinical isolates of *P. aeruginosa* [52, 53]. In addition, it was found to have the capacity to promote re-epithelialization of an injured area produced in a monolayer of keratinocytes (i.e. the most abundant cells in the epidermis) [54], at a faster rate than the mammalian AMP LL-37 [31]. Here, for the first time, we produced Esc(1-21)-coated AuNPs and investigated their antipseudomonal and cytotoxic properties along with the underlying mode of action, as well as their ability to stimulate migration of human keratinocytes in an *in vitro* pseudo-"wound" healing assay.

2. Materials and Methods

2.1. Materials

Dulbecco's modified Eagle's medium (DMEM), heat-inactivated fetal bovine serum (FBS), glutamine and gentamycin were from Euroclone (Milan, Italy); Sytox Green was obtained from Molecular Probes (Leiden, The Netherlands); 3(4,5-dimethylthiazol-2yl)2,5-diphenyltetrazolium bromide (MTT) and trypsin from bovine pancreas were from Sigma-Aldrich (St. Luis, MO). All other chemicals were reagent grade.

2.2. Peptides synthesis

Synthetic Esc(1-21) was purchased from Selleck Chemicals (Houston, TX, USA). Briefly, the peptide was assembled by step-wise solid-phase synthesis by a standard F-moc strategy and purified by reverse-phase high-performance liquid chromatography (RP-HPLC) on a semipreparative C18-bonded silica column (Kromasyl, 5 µm, 100 Å, 25 cm × 4.6 mm) using a gradient of acetonitrile in 0.1% aqueous trifluoroacetic acid at a flow rate of 1.0 mL/min, according to what reported previously [52]. Analytical RP-HPLC indicated a purity >98%. The molecular mass was verified by using MALDI-TOF Voyager DE (Applied Biosystems) [51].

2.3. Synthesis of AuNPs and their characterization

AuNPs with an average diameter of ~14 nm were synthesized by the citrate reduction method as previously described [55, 56]. Briefly, hydrogen tetrachloroaureate (III) (0.08 g; 0.235 mmol) was dissolved in 200 mL of Milli-Q water and magnetically stirred under reflux. Sodium citrate dihydrate (0.240 g; 0.81 mmol) was added, and the solution was kept under ebullition and protected from light for 30 min. The synthesized AuNPs were characterized by Ultraviolet-visible spectroscopy (UV-Vis) (Cary 100, Agilent) due to their surface plasmon resonance (λmax, 519 nm) and by transmission electron microscopy (TEM, FEI Tecnai T20). To determine the particle concentration, a molar extinction coefficient (λ = 450) of 1.76 x 10^8 was used [57]. To further stabilize the AuNPs, a bifunctional poly(ethylene glycol) (PEG) was used [50]. Briefly, 0.5 nmol of citrate AuNPs, 2.6 µmol SH-EG(8)-$(CH_2)_2$-COOH and 0.028% sodium dodecyl sulfate were mixed in a final volume of 50 mL of water. Sodium hydroxide was further added to a final concentration of 25 mM. The mixture was incubated for 16 h at room temperature, and the excess of PEG chains removed by centrifugation at 14,000 x g for 30 min at 4 °C, thrice. Twenty pmol of AuNPs conjugated to PEG (AuNPs@PEG) were incubated with different amounts and ratios of 1-Ethyl-3-(3-dimethylaminopropyl)-carbodiimide) (EDC) and N-hydroxysulfosuccinimide (Sulfo-NHS) in 1 mL of 10 mM 2-(N-morpholino)ethanesulfonic acid (MES), pH 6.1. Following 30 min of

incubation, the excess of reagents was removed by centrifugation at 16,000 x g and the AuNPs@PEG resuspended in 1 mL of MES. The aggregation of the AuNPs@PEG was assessed by UV-Vis and the best condition to maintain AuNPs@PEG stability and to avoid their aggregation was selected for further experiments (2.5 µmols of EDC and 4.6 µmols of Sulfo-NHS) (Refer to Fig. S1 and Table S1). Once the AuNPs@PEG were activated using EDC and sulfo-NHS, a different amount of the cationic Esc(1-21) peptide (from 1.5 µg to 4 µg) was added to the mixture and incubated in 10 mM MES pH 6.5 at room temperature for 2 h. After coupling, AuNPs@Esc(1-21) were centrifuged at 16,000 x g for 30 min at 4 °C to wash the excess of peptide. The AuNPs@Esc(1-21) were resuspended in 1 mL of water. The stability of AuNPs@Esc(1-21) was assessed again by UV-Vis and the amount of 2 µg of peptide was chosen for all the experiments. The supernatant was recovered and analyzed for the amount of Esc(1-21) by the colorimetric microBCA protein assay reagent kit (Pierce, Rockford IL), according to the manufacture instructions, using a standard curve of Esc(1-21). The range of linearity of the assay was from 0 µg/mL to 10 µg/mL peptide concentration. The collected supernatant was centrifuged at 14,000 x g for 30 min in order to remove any AuNP that could interfere in the assay. A reference solution was prepared with the initial peptide concentration at the same reaction conditions.

The amount of peptide in the supernatant (not attached to the AuNPs@PEG) was measured. Therefore, by knowing the added peptide (reference solution) it was possible to correlate by difference the amount of peptide bound to the AuNPs@PEG. All measurements were carried out in triplicate. Knowing the amount of AuNPs@PEG that were used for each immobilization (20 pmols) and the amount of peptide that was conjugated (0.7 µg of peptide), it was possible to calculate the number of peptides per AuNP@PEG using the Avogadro constant. To evaluate the charge of the functionalized AuNPs@Esc(1-21) compared to AuNPs@PEG, ζ-potential was performed on a Malvern Zetasizer instrument at 25 °C.

2.4. *Microorganisms and cell line*

The microorganism used in our experiments as a reference strain of *P. aeruginosa* was the standard non mucoid ATCC 27853 [58]. The well-established human immortalized keratinocytes cell line (HaCaT [59]) were used throughout the study.

2.5. *Antimicrobial activity*

Bacteria were grown in Luria-Bertani (LB) broth at 37 °C till a mid-log phase which was aseptically monitored by absorbance at 590 nm (A_{590nm}= 0.8) with an UV-1700 Pharma Spec spectrophotometer (Shimadzu, Tokyo, Japan). Afterwards, bacterial cells were centrifuged at 1,400 x g for 10 min, washed and resuspended in 5 mL of 100 mM sodium phosphate buffer, pH 7.4 (NaPB). About 4 x 10^7 bacterial cells in a total volume of 100 µL were incubated at 37 °C with serial two-fold dilution of Esc(1-21), AuNPs@Esc(1-21) or AuNPs@PEG [final cell density of 4 x 10^8 colony forming units (CFU)/mL]. Aliquots of 5 µL were withdrawn after 20 min and diluted 1:10,000 into LB. Afterwards, 20 µL of the diluted bacterial suspension were spread onto LB-agar plates for counting after overnight incubation at 37 °C. Controls were given by buffer-treated bacterial cells. Minimal bactericidal concentration (MBC_{50}) was defined as the minimal drug concentration sufficient to cause at least 50% reduction in the number of viable bacteria within 20 min. The experiments were performed three times in triplicates. In another set of experiments, a concentration corresponding to 2 x MBC_{50} of free peptide (2 µM) or AuNPs@Esc(1-21) (10 nM) in NaPB was pre-incubated with trypsin (0.02 µg/mL) for 100 min at 37 °C under mild agitation in a volume of 50 µl. Afterwards, 50 µl of bacteria in NaPB were added to reach a final mixture volume of 100 µL and a cell density of about 4 x 10^8 CFU/mL in the presence of Esc(1-21) or AuNPs@Esc(1-21) at their MBC_{50} (1 µM and 5 nM, respectively). After 20 min treatment, aliquots were withdrawn and plated for counting. Bacteria incubated with trypsin or NaPB were also included for comparison. Note that in order to have a valid indication of the resistance of

AuNPs@Esc(1-21) to proteolytic degradation, we chose an enzyme (i.e. trypsin) that, according to the prediction of cleavage sites in Esc(1-21), is expected to cleave the peptide at multiple sites in contrast with other enzymes, such as bacterial proteases.

2.6. Antibiofilm activity

Biofilm formation was performed using the Calgary Biofilm Device (Innovotech, Innovotech Inc. Edmonton, Canada) provided with microtiter 96-well plates sealed with 96 pegs-lid. Each well contained 150 µL of the bacterial inoculum (1 x 10^7 cells/mL) in LB medium. After 20 h incubation in a humidified orbital incubator at 35 °C under mild agitation, the pegs where biofilm was formed, were rinsed twice with phosphate buffered saline (PBS) and transferred into another 96-wells plate, each well containing 200 µL of PBS supplemented or not with the free peptide, AuNPs@Esc(1-21) or AuNPs@PEG. The plate was then incubated at 37 °C for 2 h. Afterwards, pegs were washed again with PBS; each peg was broken from the lid and transferred into an eppendorf tube containing 200 µL of PBS. Samples were then sonicated three times for 10 min in an ultrasonic water bath to detach bacterial cells from the pegs. Aliquots were plated on LB-agar plates for the CFU counting. The number of viable bacteria was expressed as a percentage with respect to the control (buffer-treated biofilm). The minimal biofilm eradication concentration ($MBEC_{50}$) was defined as the lowest drug concentration sufficient to cause at least 50% killing of biofilm cells within 2 h. The experiments were performed three times in triplicates.

2.7. Membrane permeabilization

The ability of AuNPs@Esc(1-21) to affect the membrane permeability of *P. aeruginosa* cells, as previously found for the free peptide [52] was assessed by the Sytox Green assay in microtiter plates. Briefly, about 2 x 10^7 bacterial cells in 50 µL of NaPB supplemented with 1 µM Sytox Green were added to each well. Then, 5 µL of AuNPs@Esc(1-21), AuNPs@PEG or free Esc(1-21) were

added. For the control sample, 5 µL of peptide solvent (water) were used. The increase in fluorescence, owing to the binding of the dye to intracellular DNA, was measured every min for 30 min at 37 °C with a microplate reader (Infinite M200; Tecan, Salzburg, Austria) at excitation and emission wavelengths equal to 485 and 535 nm, respectively. Considering the absorbance of AuNPs@PEG as a background, we properly subtracted the measurements of these samples from those containing AuNPs@Esc(1-21). Final values were reported as ratio of each value (measured within 30 min) to the initial one measured after 1 min.

2.8. Scanning electron microscopy (SEM)

P. aeruginosa was grown overnight at 37 °C in LB. After 10 min centrifugation at 1,400 x g, the bacterial pellet was resuspended in NaPB to an optical density of 0.8 at 590 nm. The bacterial culture was passed through a syringe to avoid possible clumps. Approximately 4 x 10^7 bacterial cells in a total volume of 100 µL were incubated with AuNPs@Esc(1-21) or AuNPs@PEG at 37 °C in a thermomixer under agitation for different times (1 min, 8 min and 15 min). Controls were buffer-treated bacterial cells. At the indicated time intervals, samples were centrifuged at 6,000 x g for 10 min and washed three times with NaPB. Afterwards, they were fixed with 2.5% glutaraldehyde (100 µL) in NaPB for 2 h at room temperature. The samples were then centrifuged at 12,000 x g for 10 min and washed three times as above. Samples were analyzed using an Environmental scanning electron microscope (ESEM, Quanta FEG 250) with a wet scanning-transmission electron microscopy (wet-STEM) detector at high vacuum mode. Specimens were mounted in a Quantifoil® holey carbon film copper grids and examined with a working distance between 7-10 mm and an accelerating voltage of 20 kV.

2.9. Transmission Electron Microscopy (TEM)

Bacterial samples were similarly prepared as described in the above paragraph for SEM analysis, and treated with AuNPs@Esc(1-21) for 15 min. Approximately 4 x 10^8 bacterial cells in a total

volume of 1 mL NaPB were incubated with AuNPs@Esc(1-21) for 15 min in the thermomixer with agitation. Controls were buffer-treated bacteria. After incubation, the samples were centrifuged at 6,000 x g for 10 min and washed three times with NaPB, fixed with 2.5% glutaraldehyde (1 mL) in NaPB for 2 h at room temperature. Finally, the samples were centrifuged at 12,000 x g for 10 min and washed three times as above. The pellets were subsequently embedded in 1.5 % agar (Panreac); post fixed in 2% osmium tetroxide for 1 h at room temperature and stained in 1% uranyl acetate in the dark for 2 h at 4 °C. Then, they were rinsed in distilled water, dehydrated in ethanol and infiltrated overnight in Durcupan resin (Fluka). Following polymerization, embedded cultures were detached from the wells and glued to araldite blocks. Finally, ultra-thin sections (0.08 µm) were cut with a diamond knife (Leica), stained with lead citrate (Reynolds solution) and examined under a 200 keV transmission electron microscope FEI Tecnai T20 (FEI Europe) operating at 60 keV.

2.10. Cytotoxicity

The effect of non-conjugated or functionalized AuNPs@Esc(1-21) on the viability of mammalian keratinocytes was determined by the MTT assay [51, 60]. Keratinocytes were cultured in DMEM supplemented with 10% FBS, glutamine (4 mM) and 0.05 mg/mL gentamicin, at 37 °C and 5% CO_2, in 25-cm^2 flasks.

Keratinocytes were plated in triplicate wells of a microtiter plate, at 4 x 10^4 cells/well in DMEM supplemented with 4 mM glutamine (DMEMg) and 2% FBS without antibiotic. After overnight incubation at 37 °C and 5% CO_2 atmosphere, the medium was replaced with 100 µl fresh DMEMg containing the NPs at different concentrations. Controls were cells incubated with DMEMg in the presence of peptide solvent (water). The plate was incubated for 2 h or 24 h at 37 °C and 5% CO_2 atmosphere. Afterwards, DMEMg was removed and each well was washed three times with Hank's buffer and 100 µL of Hank's buffer containing 0.5 mg/mL MTT were added to each one. After 4 h incubation, the formazan crystals were dissolved by adding 100 µL of acidified isopropanol [31]

and absorbance of each well was measured at 570 nm using the microplate reader. Cell viability was calculated with respect to the control according to the formula:

$$\frac{\text{Absorbance}_{\text{sample}} - \text{Absorbance}_{\text{blank}}}{\text{Absorbance}_{\text{control}} - \text{Absorbance}_{\text{blank}}} \text{ X } 100$$

where the blank is given by samples without cells and not treated with the peptide or NPs.

2.11. Cell migration assay

The ability of AuNPs@Esc(1-21) to stimulate migration of keratinocytes was studied according to a modified scratch assay [31-33]. Briefly, HaCaT cells (4×10^4) suspended in DMEMg supplemented with 10% FBS were seeded on each side of an ibidi culture insert for live cell analysis (Ibidi, Munich, Germany). Inserts were placed into wells of a 24-wells plate and incubated at 37 °C and 5% CO_2 to allow cells grow to confluence. Afterwards, inserts were carefully removed to create a cell-free area (pseudo-"wound") of approximately 500 µm, and 300 µl of DMEMg supplemented with AuNPs@Esc(1-21) or AuNPs@PEG or the free peptide, were added. Control samples were cells treated with DMEMg in the presence of peptide solvent (water). Cells were allowed to migrate for 9 h in an appropriate incubator. All experiments were run in triplicates. At different time intervals, fields of the pseudo-"wound" area were visualized under an inverted microscope (Olympus CKX41) at x 4 magnification and photographed with a Color View II digital camera. The percentage of cell-covered area at each time was determined by WIMASIS Image Analysis program.

2.12. Statistical analysis

Quantitative data were expressed as the mean ± SEM. Statistical analysis was performed using two-way analysis of variance (ANOVA), with PRISM software (GraphPad, San Diego, CA).

Differences were considered to be statistically significant for $p< 0.05$. The levels of statistical significance are indicated in the legend to figures.

3. Results

3.1. AuNPs synthesis characterization

AuNPs were synthesized by citrate reduction of gold [55, 56]. The AuNPs exhibited a maximum peak of absorption at 519 nm and had an average size of 14 nm as visualized by TEM (Fig. 1). To increase the stability of the AuNPs to salt and further centrifugation steps, a bifunctional PEG was used [SH-EG(8)-$(CH_2)_2$-COOH] [50]. This PEG replaces the citrate molecules and binds to the NPs surface *via* a gold-thiol bond (AuNPs@PEG). Importantly, it also provides a carboxylic group, for further derivatization with the peptide *via* carbodiimide-mediated coupling. In order to attach the peptide, the carboxylic groups of the AuNPs@PEG were activated with different amounts and ratios of EDC and sulfo-NHS (Table S1) [61] and the stability of the nanoparticles was assessed by UV-Vis spectroscopy (Fig. S1). Once selected the amount of EDC and sulfo-NHS that did not alter the stability of the AuNPs@PEG, different amounts of peptide were added to the same amount of activated AuNPs@PEG. The stability was checked once again by UV-Vis spectroscopy. From these data, 2 μg of Esc(1-21) was selected as the maximum amount of peptide that could be added without causing precipitation of the negatively-charged AuNPs@PEG during the coupling process (Fig. S2).

After coupling, the AuNPs@Esc(1-21) were centrifuged and the supernatant was recovered for peptide quantification (as indicated in the Experimental section): 0.7 μg of peptide resulted to be bound to 20 pmol of AuNPs@PEG, resulting in about 16 molecules of peptide per AuNP@PEG. Both AuNPs@PEG and AuNPs@Esc(1-21) were characterized by TEM (Fig. 1), UV-Vis spectroscopy (Fig. S2 B) and ζ-potential. The slight decrease in the ζ-potential of functionalized AuNPs@Esc(1-21) (-35.58 mV) compared to AuNPs@PEG (-39.44 mV) is in accordance with the

covalent conjugation of a positively-charged molecule (i.e. the cationic peptide) to the negatively-charged AuNPs@PEG. Table 1 summarizes the comparison between different molar concentrations of AuNPs@Esc(1-21) used in our experiments and the corresponding molar concentration of peptide bound to them.

3.2. AuNPs@Esc(1-21) are more active than the free peptide against P. aeruginosa

It was previously demonstrated that Esc(1-21) provokes, within 15 min, 3-$\log_{10}$ reduction in the number of viable bacterial cells (99.9% killing) of the reference strain *P. aeruginosa* ATCC 27853 when added at 1 μM to 1 x 10^6 CFU/mL in physiological solution [52]. When the peptide was assayed in NaPB at a concentration range from 4 μM to 0.1 μM against a higher cell density i.e. 4 x 10^8 CFU/mL, which was needed to prepare samples for electron microscopy analysis (see next paragraphs), a clear dose-dependent bacterial cell death was detected (Fig. 2A). The minimal bactericidal concentration sufficient to cause at least 50% decrease in the number of CFU (MBC_{50}) within 20 min was of 1 μM (Table 2). Interestingly, when Esc(1-21) was coated onto AuNPs@PEG, it was found not only to preserve a concentration-dependent microbicidal effect (Fig. 2B), but also to exhibit a significantly higher killing activity, with ~12-fold lower MBC_{50} (0.08 μM, see Table 2). Note that this peptide concentration was equivalent to that of 5 nM AuNPs@Esc(1-21) (Table 1). Importantly, when AuNPs@Esc(1-21) were centrifuged after 24 h incubation at 37 °C, no antimicrobial activity was observed in the supernatant (data not shown) which indicates that the peptide is not detached from the NPs surface.

According to the reported literature [62], no lethal activity was displayed by AuNPs@PEG.

Remarkably, when AuNPs@Esc(1-21) were tested against the sessile form of *P. aeruginosa*, 50% killing of biofilm cells was recorded within 2 h treatment (Table 2), at a concentration of coated-peptide (0.17 μM) which was only 2-fold higher than the MBC_{50}, and about 17-fold lower than the $MBEC_{50}$ of the free peptide (3 μM). No biofilm eradication was manifested by AuNPs@PEG.

3.3. AuNPs@Esc(1-21) preserve their antibacterial activity in the presence of a proteolytic enzyme

In addition, AuNPs@Esc(1-21) were found to retain their antibacterial activity in the presence of trypsin. In fact, when the free peptide or the AuNPs@Esc(1-21) were used at their MBC_{50} after pre-treatment with trypsin at significantly lower physiological concentration [63], only ~13% killing of bacteria was observed for Esc(1-21) (Fig. 3) which corresponds to about 4-fold reduction of activity compared to that of the free peptide at its MBC_{50} (1 μM) without pre-treatment (Fig. 2). In contrast, no significant change in the bactericidal activity was caused by pre-incubation of AuNPs@Esc(1-21) with trypsin (Fig. 3). This is likely due to a higher resistance of Esc(1-21) to enzymatic degradation upon its coating to AuNPs@PEG compared to its soluble free form.

3.4. AuNPs@Esc(1-21) have a membrane-perturbing activity

In order to know whether a membrane-perturbing activity was the major killing mechanism of AuNPs@Esc(1-21), in line with what described for the free Esc(1-21) peptide [52], the Sytox Green assay on the planktonic form of *P. aeruginosa* was performed at a concentration of functionalized AuNPs@Esc(1-21) giving rise to approximately 70% bacterial death, i.e. 10 nM (Fig. 2B). Sytox Green is a membrane-impermeable probe whose fluorescence intensity dramatically enhances upon binding to DNA, once it has entered cells with a damaged cytoplasmic membrane. A clear membrane disturbance was induced by AuNPs@Esc(1-21), as pointed out by the fast increase of fluorescence intensity immediately after their addition to the bacteria, reaching a maximum effect within 15-20 min (Fig. 4) in accordance to the kinetics of membrane perturbation previously shown by concentrations of the free peptide causing a similar percentage of *Pseudomonas* killing (~70 %) [52]. Note that when a concentration of free Esc(1-21) corresponding to the amount of peptide bound to 10 nM AuNPs@Esc(1-21) was used (0.17 μM), no significant alteration of membrane

permeability was detected, as indicated by the invariant fluorescent signal of the sample (Fig. 4). This is in line with the significantly lower antipseudomonal activity of Esc(1-21) at this concentration (data not shown).

3.5. AuNPs@Esc(1-21) destroy the cellular structure of P. aeruginosa (electron microscopy analysis)

The effect of AuNPs@Esc(1-21), when used at their MBC_{50} on the morphology of the planktonic form of *P. aeruginosa* ATCC 27853 after different incubation times was visualized by electron microscopy. As highlighted by SEM analysis (Fig. 5), AuNPs@Esc(1-21) appeared to be concentrated on the microbial surface already after 1 min incubation with the bacteria, while AuNPs@PEG could not be detected (Fig. 5, left panels). The magnified area in Fig. 5 (left side) shows that AuNPs@Esc(1-21) formed clusters attached to the cell membrane at various points, but without compromising the cell integrity. This outcome became more pronounced after 8 min treatment with AuNPs@Esc(1-21) (Fig. 5, right panels) and was accompanied by membrane breakages leading to leakage of intracellular material (Fig. 5, arrows). These results are comparable to those previously obtained with the free peptide [52]. In contrast, both the control and AuNPs@PEG-treated samples were shown to retain their cellular integrity and only very rarely did the AuNPs@PEG appear within *Pseudomonas* cells (Fig. 5). Furthermore, 15 min after treatment with functionalized AuNPs@Esc(1-21), a drastic change in the bacterial shape with a marked disintegration of the cellular structure were visualized in some bacteria compared to the control, as indicated by TEM analysis (Fig. 6).

Overall, in combination with the results of the Sytox Green assay described above this additional data support the notion that conjugation of Esc(1-21) to AuNPs@PEG does not affect the well-established membrane-perturbing activity of the peptide [52].

3.6. AuNPs@Esc(1-21) are not toxic to human keratinocytes

The impact of AuNPs@Esc(1-21) on the viability of human keratinocytes was determined by the MTT assay on HaCaT cells. Both AuNPs@Esc(1-21) and AuNPs@PEG did not induce any cytotoxic effect, being unable to reduce the number of metabolically active cells up to the highest concentration used (60 nM) corresponding to 12 x MBC_{50} (Fig. 7). This is in agreement with published papers showing no toxicity for AuNPs [62] or Esc(1-21) up to 64 µM [31]. Note that when AuNPs@Esc(1-21) were incubated with HaCaT cells for a longer time (24 h) at the highest concentration used (60 nM), ~97 % cell viability was recorded.

3.7. AuNPs@Esc(1-21) stimulate migration of HaCaT cells

Finally, to explore whether our functionalized AuNPs were able to retain the ability of the free peptide to induce re-epithelialization by migrating HaCaT cells [31], a pseudo-"wound" healing assay was carried out. As illustrated in Fig. 8, while non-coated AuNPs@PEG had not effect on migration of keratinocytes compared to the control, 5 nM AuNPs@Esc(1-21) promoted the closure of the pseudo-"wound" field created in the HaCaT monolayer, with a similar rate to that displayed by a 3-fold higher concentration of free Esc(1-21), i.e. 0.25 µM.

4. Discussion

Epithelial infections by *P. aeruginosa* are actually very difficult to eradicate, mainly due to the intrinsic resistance of this microbial pathogen to the currently used drugs, as well as to its propensity to grow in biofilm communities protecting bacterial cells from a large diversity of environmental insults [64]. *Pseudomonas* biofilm can easily colonize skin ulcers, mostly in diabetic patients or patients with venous or arterial disease, as well as surgical wounds; and has become a relevant cause of morbidity and mortality, particularly in hospitalized individuals [65-67].

Nowadays AMPs hold promise as a valid alternative for new anti-infective agents with expanding properties [3]. Nevertheless, the limited strategies to enhance their half-life and to deliver them to the correct site of infection, without altering the antimicrobial/biological properties of the peptide, have contributed to complicate and slow down their clinical translation. As emphasized by numerous reports in the literature, AuNPs have revolutionized the field of bio-nanomedicine [68]. The application of AuNPs has increased dramatically over the last two decades due to the rapid progress of nanoscale analytical tools [69]. Because of their small size, high solubility and vast surface area, they can carry a relatively high drug dose [70], thus enhancing its interaction with the target cell. Note that non-functionalized AuNPs were shown to be harmless to biological systems, due to gold elemental properties, including biocompatibility and chemical inertness (stability/low reactivity) [71-77]. It is worthwhile recalling that the previously reported antibacterial activity of AuNPs could be due to co-existing chemicals involved in the synthesis of these NPs but not completely removed from them [78]. Recent studies have highlighted an antibacterial activity of AuNPs, once stabilized with a capping agent (polyelectrolyte poly-allylaminehydrochloride, PHA), which would favor self-assembly of AuNPs into long chains speeding up the cell wall breakdown and cytoplasm release [79].

Furthermore, combination of conventional antibiotics e.g. ceftriazone with AuNPs has already manifested a six-fold higher effectiveness in killing a variety of bacterial species than the drug alone [80]. Yet, the synthesis of sugar residues containing cyclic cationic peptides attached to AuNPs was found to show an antimicrobial activity comparable to that of the free peptides [81]. Only very lately, an antibacterial activity was demonstrated by a synthetic AMP (i.e. cecropin-melittin hybrid) when immobilized on AuNPs-coated surfaces to be translated into biomedical materials [82] or when used to synthesize AuNPs [83].

Here, by employing a derivative of the frog skin AMP esculentin-1a, Esc(1-21), we demonstrated a remarkably improved antibacterial activity of an AMP chemically conjugated to AuNPs *via* PEG linker compared to the activity explicated by the same concentration of the free peptide. This is

likely due to the considerable quantity of Esc(1-21) lining the surface of AuNPs@PEG, regardless of its orientation, and to the high concentration of AuNPs@Esc(1-21) on the bacterial surface as well as to the prolonged bioavailability of the peptide, being less accessible to bacterial proteases. This would ensure a much higher local concentration of Esc(1-21) at the site of bacterium-NP contact. Furthermore, by means of the Sytox Green assay and electron microscopy techniques we were able to prove that, likewise to the free Esc(1-21), the functionalized AuNPs@Esc(1-21) do possess a membrane perturbing activity as a plausible mechanism of bacterial killing. Interestingly, non-coated AuNPs@PEG were not detected on the surface of *Pseudomonas* cells. This points out that the cationic Esc(1-21) is the driving force allowing AuNPs@Esc(1-21) to target bacterial cells, by presumably recognizing and interacting with the negatively-charged cell surface components, lipopolysaccharides. Owing to this interaction, the killing of bacterial cells through a membrane disruption process, would take place without intracellular entry of AuNPs@Esc(1-21), according to what found for the cationic PHA-AuNPs [84], as well as for the AuNPs containing a hexyl-substituted ammonium-functionalized thiol as a protective coating [85, 86]. A schematic representation of the behavior of both AuNPs@PEG and AuNPs@Esc(1-21) on the bacterium *P. aeruginosa* is sketched in Fig. 9.

Another outstanding matter is that similarly to what recorded for the free Esc(1-21), we were able to demonstrate that AuNPs@Esc(1-21) also stimulate cells migration in a pseudo-"wound" healing assay on a monolayer of keratinocytes, suggesting their propensity to accelerate recovery of an injured skin layer, following bacterial infection.

To the best of our knowledge, this is the first report showing that covalent conjugation of a linear membrane-active AMP to soluble AuNPs, *via* a PEG linker, dramatically increases antibacterial/antibiofilm activities against one of the most diffused nosocomial pathogens , i.e. *P. aeruginosa*, without being noxious. As mentioned above, recent studies showed an antipseudomonal activity by the cecropin-melittin AMP when covalently bound to surface-tethered AuNPs. However, an extremely high concentration of coated peptide (110 μg/cm^2 corresponding to

~2 mM peptide in solution) was needed to cause 70% killing of bacterial cells within 2 h [82]. In addition, the minimal growth inhibitory concentration of immobilized peptide was found to be 8-9 times higher than that of the soluble AMP [82]. Furthermore, in the paper from Rai and colleagues [83], it was demonstrated that when the cecropin-melittin AMP was functionalized onto citrate AuNPs, only a very slight antibacterial activity was exhibited (less than 10% killing of the Gram-negative bacterium *Escherichia coli*) and that the obtained NPs precipitated in less than one hour. Only when cecropin-melittin AuNPs were prepared by a one-pot methodology, they were able to display a relative antibacterial activity, although eight days were required to produce such NPs [83]. More specifically, 1,25 μg/mL of immobilized cecropin-melittin peptide (~0,7 μM) was necessary to kill approximately ~10^5 *E. coli* cells in 1 h, whereas in our case ~ 10^7 cells of the widely feared *Pseudomonas* pathogen were eliminated within 20 min by 5 nM AuNPs@Esc(1-21) corresponding to 0.08 μM of coated-peptide (Table 1). In addition, we have found that AuNPs@PEG functionalized with Esc(1-21) do not precipitate within months. Obtaining peptides that maintain their activity after immobilization and that are stable over time is of the utmost importance thinking on clinic translation opportunities.

On the whole, our results suggest Esc(1-21)-coated AuNPs@PEG to be a valuable and advantageous therapeutic solution for local treatment of skin infections. In support of this hypothesis, it was demonstrated recently that AuNPs can pass through different types of animal tissues and that diffusion through the stratum corneum barrier of intact human and mouse skin is influenced by their size, shape and charge [87]. In an *in vitro* diffusion cell system, AuNPs have been found to penetrate all layers of human skin [76] in greater amount than other metal NPs, i.e. silver NPs (which can be absorbed through the skin [77]), thus raising the interest for developments of AuNPs in transdermal administration of drugs and therapy.

5. Conclusions

The engineered peptide-conjugated AuNPs@PEG presented in this work have been shown to enhance by approximately 15-fold the antipseudomonal activity of the membrane-active Esc(1-21) without being toxic to human cells i.e. keratinocytes as well as to increase the peptide's re-epithelialization activity on a keratinocytes monolayer. In conclusion, these findings make our designed NPs attractive candidates for their future development as new nanoscale formulations likely for topical (dermatological) treatment of epithelial infections [88, 89]. Importantly, even though in this study we presented data of AuNPs@Esc(1-21) only against *P. aeruginosa*, we believe that our designed NPs will be biocidal against a wide range of microbial pathogens. This is corroborated by the large spectrum of antimicrobial activity of Esc(1-21) [90]; its ability to perturb anionic model membranes mimicking those of bacterial cells (manuscript in preparation) and; the capacity of its shorter analog Esc(1-18) to damage the membrane of both Gram-positive and Gram-negative bacteria [51, 91].

Future interdisciplinary studies aimed at understanding the basic rules governing molecular interactions between such coated-AuNPs and cells or complex tissues e.g. the skin, will offer the possibility to rationally design new pharmacological AMP-based strategies to overcome the limited biostability, toxicity and inefficient delivery of AMPs to the target infectious site. Furthermore, combination of AMP conjugated-AuNPs with phothermal therapy is highly expected to produce advancement of nanomedicine for the local treatment of chronic infected wounds. Indeed, once irradiated by laser, AuNPs can efficiently convert photo energy into heat, causing a temperature raise in the specific target site with killing of bacteria [92].

ACKNOWLEDGMENTS

This work was supported grants from Sapienza Università di Roma and ERC-Starting Grant 239931- NANOPUZZLE, SAF2014-54763-C2-2-R, and Research Funding from DGA (Fondo Social Europeo).

REFERENCES

1. H.W. Boucher, G.H. Talbot, J.S. Bradley, J.E. Edwards, D. Gilbert, L.B. Rice, M. Scheld,B. Spellberg, J. Bartlett. Bad bugs, no drugs: no ESKAPE! An update from the Infectious Diseases Society of America. Clin Infect Dis. 48 (2009) 1-12
2. WHO. WHO Antimicrobial Resistance, Global Report on Surveillance 2014 (2014) 257
3. J. Fernebro. Fighting bacterial infections-future treatment options. Drug Resist Updat. 14 (2011) 125-139
4. J. Lakshmaiah Narayana, J.Y. Chen. Antimicrobial peptides: Possible anti-infective agents. Peptides.72 (2015) 88-94
5. M. Zasloff. Antimicrobial peptides of multicellular organisms. Nature. 415 (2002) 389-395
6. H.G. Boman. Gene-encoded peptide antibiotics and the concept of innate immunity: an update review. Scand J Immunol. 48 (1998) 15-25
7. K.A. Brogden. Antimicrobial peptides: pore formers or metabolic inhibitors in bacteria? Nat Rev Microbiol. 3 (2005) 238-250
8. B. Schittek, R. Hipfel, B. Sauer, J. Bauer, H. Kalbacher, S. Stevanovic, M. Schirle, K. Schroeder, N. Blin, F. Meier, G. RassnerC. Garbe. Dermcidin: a novel human antibiotic peptide secreted by sweat glands. Nat Immunol. 2 (2001) 1133-1137

9. J. Harder, J.M. Schroder. Antimicrobial peptides in human skin. Chem Immunol Allergy. 86 (2005) 22-41

10. R. Lai, H. Liu, W. Hui Lee,Y. Zhang. An anionic antimicrobial peptide from toad *Bombina maxima*. Biochem Biophys Res Commun. 295 (2002) 796-799

11. M.L. Mangoni. A lesson from Bombinins H, mildly cationic diastereomeric antimicrobial peptides from Bombina skin. Curr Protein Pept Sci. 14 (2013) 734-743

12. L.J. Zhang,R.L. Gallo. Antimicrobial peptides. Curr Biol. 26 (2016) R14-19

13. A.C. Seefeldt, M. Graf, N. Perebaskine, F. Nguyen, S. Arenz, M. Mardirossian, M. Scocchi, D.N. Wilson, C.A. Innis. Structure of the mammalian antimicrobial peptide Bac7(1-16) bound within the exit tunnel of a bacterial ribosome. Nucleic Acids Res. 44 (2016) 2429-2438

14. M. Mardirossian, R. Grzela, C. Giglione, T. Meinnel, R. Gennaro, P. Mergaert, M. Scocchi. The host antimicrobial peptide Bac71-35 binds to bacterial ribosomal proteins and inhibits protein synthesis. Chem Biol. 21 (2014) 1639-1647

15. K.Y. Choi, L.N. Chow, N. Mookherjee. Cationic host defence peptides: multifaceted role in immune modulation and inflammation. J Innate Immun. 4 (2012) 361-370

16. A.T. Yeung, S.L. Gellatly, R.E. Hancock. Multifunctional cationic host defence peptides and their clinical applications. Cell Mol Life Sci. 68 (2011) 2161-2176

17. S.C. Mansour, O.M. Pena, R.E. Hancock. Host defense peptides: front-line immunomodulators. Trends Immunol. 35 (2014) 443-450

18. M.L. Mangoni, A. Carotenuto, L. Auriemma, M.R. Saviello, P. Campiglia, I. Gomez-Monterrey, S. Malfi, L. Marcellini, D. Barra, E. Novellino, P. Grieco. Structure-activity relationship, conformational and biological studies of temporin L analogues. J Med Chem. 54 (2011) 1298-1307

19. M.L. Mangoni, A. Di Grazia, F. Cappiello, B. Casciaro, V. Luca. Naturally occurring Peptides from *Rana temporaria*: Antimicrobial Properties and More. Curr Top Med Chem. 16 (2015) 54-64

20. C. Song, C. Weichbrodt, E.S. Salnikov, M. Dynowski, B.O. Forsberg, B. Bechinger, C. Steinem, B.L. de Groot, U. Zachariae, K. Zeth. Crystal structure and functional mechanism of a human antimicrobial membrane channel. Proc Natl Acad Sci U S A. 110 (2013) 4586-4591

21. C.D. Fjell, J.A. Hiss, R.E. Hancock,G. Schneider. Designing antimicrobial peptides: form follows function. Nat Rev Drug Discov. 11 (2012) 37-51

22. L.T. Nguyen, E.F. Haney, H.J. Vogel. The expanding scope of antimicrobial peptide structures and their modes of action. Trends Biotechnol. 29 (2011) 464-472

23. M.L. Mangoni,V. Luca, A.M. McDermott. Fighting microbial infections: A lesson from amphibian skin-derived esculentin-1 peptides. Peptides. *71* (2015) 286-295

24. M.L. Mangoni, Y. Shai. Short native antimicrobial peptides and engineered ultrashort lipopeptides: similarities and differences in cell specificities and modes of action. Cell Mol Life Sci. 68 (2011) 2267-2280

25. J.L. Fox. Antimicrobial peptides stage a comeback. Nat Biotechnol. 31 (2013) 379-382

26. D.C. Wu, W.W. Chan, A.I. Metelitsa, L. Fiorillo, A.N. Lin. *Pseudomonas* skin infection: clinical features, epidemiology, and management. Am J Clin Dermatol. 12 (2011) 157-169

27. T.F. Mah, B. Pitts, B. Pellock, G.C. Walker, P.S. Stewart,G.A. O'Toole. A genetic basis for *Pseudomonas aeruginosa* biofilm antibiotic resistance. Nature. 426 (2003) 306-310

28. P.K. Taylor,A.T. Yeung, R.E. Hancock. Antibiotic resistance in *Pseudomonas aeruginosa* biofilms: towards the development of novel anti-biofilm therapies. J Biotechnol. 191 (2014) 121-130

29. Y. Morita, J. Tomida, Y. Kawamura. Resistance and response to anti-pseudomonas agents and biocides, in Pseudomonas: New aspects of *Pseudomonas* biology, eds Ramos J., Goldberg J. B., Filloux A., editors. (New York, NY: Springer). (2015) 173-187

30. K. Poole. *Pseudomonas aeruginosa:* resistance to the max. Front Microbiol. 2 (2011) 65

31. A. Di Grazia, F. Cappiello, A. Imanishi, A. Mastrofrancesco, M. Picardo, R. Paus, M.L. Mangoni. The frog skin-derived antimicrobial peptide esculentin-1a(1-21)NH2 promotes the

migration of human HaCaT keratinocytes in an EGF receptor-dependent manner: a novel promoter of human skin wound healing? PLoS One. 10 (2015) e0128663

32. A. Di Grazia, V. Luca, L.A. Segev-Zarko, Y. Shai, M.L. Mangoni. Temporins A and B stimulate migration of HaCaT keratinocytes and kill intracellular *Staphylococcus aureus*. Antimicrob Agents Chemother. 58 (2014) 2520-2527

33. A. Di Grazia, F. Cappiello, H. Cohen, B. Casciaro, V. Luca, A. Pini, Y.P. Di,Y. Shai, M.L. Mangoni. D-Amino acids incorporation in the frog skin-derived peptide esculentin-1a(1-21)NH is beneficial for its multiple functions. Amino Acids. 47 (2015) 2505-2519

34. A.J. Huh, Y.J. Kwon. "Nanoantibiotics": a new paradigm for treating infectious diseases using nanomaterials in the antibiotics resistant era. J Control Release. 156 (2011) 128-145

35. R.Y. Pelgrift, A.J. Friedman. Nanotechnology as a therapeutic tool to combat microbial resistance. Adv Drug Deliv Rev. 65 (2013) 1803-1815

36. I. Sondi, B. Salopek-Sondi. Silver nanoparticles as antimicrobial agent: a case study on *E. coli* as a model for Gram-negative bacteria. J Colloid Interface Sci. 275 (2004) 177-182

37. G. Chen, H. Qiu, P.N. Prasad, X. Chen. Upconversion nanoparticles: design, nanochemistry, and applications in theranostics. Chem Rev. 114 (2014) 5161-5214

38. J.A. Webb, R. Bardhan. Emerging advances in nanomedicine with engineered gold nanostructures. Nanoscale. 6 (2014) 2502-2530

39. T. Vo-Dinh, A.M. Fales, G.D. Griffin, C.G. Khoury, Y. Liu, H. Ngo, S.J. Norton, J.K. Register, .N. Wang, H. Yuan. Plasmonic nanoprobes: from chemical sensing to medical diagnostics and therapy. Nanoscale. 5 (2013) 10127-10140

40. V. Raffa, O. Vittorio, C. Riggio, A. Cuschieri. Progress in nanotechnology for healthcare. Minim Invasive Ther Allied Technol. 19 (2010) 127-135

41. A.P. Jallouk, R.U. Palekar, H. Pan, P.H. Schlesinger, S.A. Wickline. Modifications of natural peptides for nanoparticle and drug design. Adv Protein Chem Struct Biol. 98 (2015) 57-91

42. J.G. Leid, A.J. Ditto, A. Knapp, P.N. Shah, B.D. Wright, R. Blust, L. Christensen, C.B. Clemons, J.P. Wilber, G.W. Young, A.G. Kang, M.J. Panzner, C.L. Cannon, Y.H. Yun, W.J. Youngs, N.M. Seckingeret, E.K. Cope. *In vitro* antimicrobial studies of silver carbene complexes: activity of free and nanoparticle carbene formulations against clinical isolates of pathogenic bacteria. J Antimicrob Chemother. 67 (2012) 138-148

43. A. Kumar, S.S. Kolar, M. Zao, A.M. McDermott, C. Cai. Localization of antimicrobial peptides on polymerized liposomes leading to their enhanced efficacy against *Pseudomonas aeruginosa.* Mol Biosyst. 7 (2011) 711-713

44. S. Ashraf, B. Pelaz, P. del Pino, M. Carril, A. Escudero, W.J. Parak, M.G. Soliman, Q. Zhang, C. Carrillo-Carrion. Gold-based nanomaterials for applications in nanomedicine. Top Curr Chem. 370 (2016) 169-202

45. H. Daraee, A. Eatemadi, E. Abbasi, S. Fekri Aval, M. Kouhi, A. Akbarzadeh. Application of gold nanoparticles in biomedical and drug delivery. Artif Cells Nanomed Biotechnol. 44 (2016) 410-422

46. R.A. Sperling, P. Rivera Gil, F. Zhang, M. Zanella, W.J. Parak. Biological applications of gold nanoparticles. Chem Soc Rev. 37 (2008) 1896-1908

47. M.C. Daniel, D. Astruc. Gold nanoparticles: assembly, supramolecular chemistry, quantum-size-related properties, and applications toward biology, catalysis, and nanotechnology. Chem Rev. 104 (2004) 293-346

48. L.R. Hirsch, N.J. Halas, J.L. West. Whole-blood immunoassay facilitated by gold nanoshell-conjugate antibodies. Methods Mol Biol. 303 (2005) 101-111

49. X. Gao,Y. Cui, R.M. Levenson, L.W. Chung, S. Nie. *In vivo* cancer targeting and imaging with semiconductor quantum dots. Nat Biotechnol. 22 (2004) 969-976

50. J. Conde, A. Ambrosone, V. Sanz, Y. Hernandez, V. Marchesano, F. Tian, H. Child, C.C. Berry, M.R. Ibarra, P.V. Baptista, C. Tortiglioneet, J.M. de la Fuente. Design of multifunctional gold nanoparticles for in vitro and in vivo gene silencing. ACS Nano. 6 (2012) 8316-8324

51. A.E. Islas-Rodriguez, L. Marcellini, B. Orioni, D. Barra, L. Stella, M.L. Mangoni. Esculentin 1-21: a linear antimicrobial peptide from frog skin with inhibitory effect on bovine mastitis-causing bacteria. J Pept Sci. 15 (2009) 607-614

52. V. Luca, A. Stringaro, M. Colone, A. Pini,M.L. Mangoni. Esculentin(1-21), an amphibian skin membrane-active peptide with potent activity on both planktonic and biofilm cells of the bacterial pathogen *Pseudomonas aeruginosa*. Cell Mol Life Sci. 70 (2013) 2773-2786

53. D. Uccelletti, E. Zanni, L. Marcellini,C. Palleschi, D. Barra, M.L. Mangoni. Anti-Pseudomonas activity of frog skin antimicrobial peptides in a *Caenorhabditis elegans* infection model: a plausible mode of action in vitro and in vivo. Antimicrob Agents Chemother. 54 (2010) 3853-3860

54. I.S. Haslam, E.W. Roubos, M.L. Mangoni, K. Yoshizato, H. Vaudry, J.E. Kloepper,D.M. Pattwell, P.F. Maderson, R. Paus. From frog integument to human skin: dermatological perspectives from frog skin biology. Biol Rev Camb Philos Soc. 89 (2014) 618-655

55. J.S. Turkevitch, P. C.; Hillier, J. A study of the nucleation and growth processes in the synthesis of colloidal gold. Discuss Faraday Soc. 11 (1951) 55-75

56. G. Frens. Controlled nucleation for the regulation of the particle size in monodisperse gold suspensions. Nature Physical Science. 241 (1973) 20-22

57. W. Haiss, N.T. Thanh, J. Aveyard, D.G. Fernig. Determination of size and concentration of gold nanoparticles from UV-vis spectra. Anal Chem. 79 (2007) 4215-4221

58. J. Li, J. Turnidge, R. Milne, R.L. Nation, K. Coulthard. *In vitro* pharmacodynamic properties of colistin and colistin methanesulfonate against *Pseudomonas aeruginosa* isolates from patients with cystic fibrosis. Antimicrob Agents Chemother. 45 (2001) 781-785

59. P. Aksoy,C.Y. Abban, E. Kiyashka, W. Qiang, P.I. Meneses. HPV16 infection of HaCaTs is dependent on beta4 integrin, and alpha6 integrin processing. Virology. 449 (2014) 45-52

60. P. Grieco, A. Carotenuto, L. Auriemma, A. Limatola, S. Di Maro, F. Merlino, M.L. Mangoni, V. Luca, A. Di Grazia, S. Gatti, P. Campiglia, I. Gomez-Monterrey, E. Novellino, A. Catania.

Novel alpha-MSH peptide analogues with broad spectrum antimicrobial activity. PLoS One. 8 (2013) e61614

61. M. Moros, S. Puertas, B. Saez, JM. de la Fuente, V. Grazú, H. Feracci. Surface engineered magnetic nanoparticles for specific immunotargeting of cadherin expressing cells. Journal of Physics D: Applied Physics. 49 (2016)

62. S. Chatterjee, A. Bandyopadhyay, K. Sarkar. Effect of iron oxide and gold nanoparticles on bacterial growth leading towards biological application. J Nanobiotechnology. 9 (2011) 34

63. L.A. Martin-Visscher, M.J. van Belkum, S. Garneau-Tsodikova, R.M. Whittal, J. Zheng, L.M. McMullen, J.C. Vederas. Isolation and characterization of carnocyclin a, a novel circular bacteriocin produced by *Carnobacterium maltaromaticum* UAL307. Appl Environ Microbiol. 74 (2008) 4756-4763

64. S.L. Percival, K.E. Hill, D.W. Williams, S.J. Hooper, D.W. Thomas, J.W. Costerton. A review of the scientific evidence for biofilms in wounds. Wound Repair Regen. 20 (2012) 647-657

65. G.D. Hannigan, N. Pulos, E.A. Grice, S. Mehta. Current concepts and ongoing research in the prevention and treatment of open fracture infections. Adv Wound Care (New Rochelle). 4 (2015) 59-74

66. T.D. Kish, M.H. Chang, H.B. Fung. Treatment of skin and soft tissue infections in the elderly: A review. Am J Geriatr Pharmacother. 8 (2010) 485-513

67. T. Mustoe. Understanding chronic wounds: a unifying hypothesis on their pathogenesis and implications for therapy. Am J Surg. 187 (2004) 65S-70S

68. M. Moros, S.G. Mitchell, V. Grazu, J.M. de la Fuente. The fate of nanocarriers as nanomedicines in vivo: important considerations and biological barriers to overcome. Curr Med Chem. 20 (2013) 2759-2778

69. M. Shah, V. Badwaik, Y. Kherde, H.K. Waghwani, T. Modi, Z.P. Aguilar, H. Rodgers, W. Hamilton, T. Marutharaj, C. Webb, M.B. Lawrenz, R. Dakshinamurthy. Gold nanoparticles: various methods of synthesis and antibacterial applications. Front Biosci. 19 (2014) 1320-1344

70. T.C. Yih, M. Al-Fandi. Engineered nanoparticles as precise drug delivery systems. J Cell Biochem. 97 (2006) 1184-1190

71. Y. Zhao,Y. Tian,Y. Cui,W. Liu,W. Ma, X. Jiang. Small molecule-capped gold nanoparticles as potent antibacterial agents that target Gram-negative bacteria. J Am Chem Soc. 132 (2010) 12349-12356

72. S.Y. Lin, N.T. Chen, S.P. Sum, L.W. Lo,C.S. Yang. Ligand exchanged photoluminescent gold quantum dots functionalized with leading peptides for nuclear targeting and intracellular imaging. Chem Commun. (2008) 4762-4764

73. A.G. Tkachenko, H. Xie, Y. Liu, D. Coleman, J. Ryan, W.R. Glomm, M.K. Shipton, S. Franzen, D.L. Feldheim. Cellular trajectories of peptide-modified gold particle complexes: comparison of nuclear localization signals and peptide transduction domains. Bioconjug Chem. 15 (2004) 482-490

74. J. Salado, M. Insausti, L. Lezama, I. Gil de Muro, M. Moros, B. Pelaz, V. Grazu, J.M. de la Fuente, T. Rojo. Functionalized Fe(3)O(4)@Au superparamagnetic nanoparticles: in vitro bioactivity. Nanotechnology. 23 (2012) 315102

75. A.N. Brown, K. Smith, T.A. Samuels, J. Lu,S.O. Obare, M.E. Scott. Nanoparticles functionalized with ampicillin destroy multiple-antibiotic-resistant isolates of *Pseudomonas aeruginosa* and *Enterobacter aerogenes* and methicillin-resistant *Staphylococcus aureus*. Appl Environ Microbiol. 78 (2012) 2768-2774

76. D.N. Williams, S.H. Ehrman, T.R. Pulliam Holoman. Evaluation of the microbial growth response to inorganic nanoparticles. J Nanobiotechnology. 4 (2006) 3

77. E.E. Connor, J. Mwamuka, A. Gole, C.J. Murphy, M.D. Wyatt. Gold nanoparticles are taken up by human cells but do not cause acute cytotoxicity. Small. 1 (2005) 325-327

78. Y. Zhang, T.P. Shareena Dasari, H. Deng, H. Yu. Antimicrobial activity of gold nanoparticles and ionic gold. J Environ Sci Health C Environ Carcinog Ecotoxicol Rev. 33 (2015) 286-327

79. Y. Zhou, Y. Kong, S. Kundu, J.D. Cirillo, H. Liang. Antibacterial activities of gold and silver nanoparticles against *Escherichia coli* and bacillus Calmette-Guerin. J Nanobiotechnology. 10 (2012) 19

80. S.A. Muhammad Raza Shah, A. Muhammad, S. Perveen, S. Ahmed, M.F. Bertinoc, M.Alib Morphological analysis of the antimicrobial action of silver and gold nanoparticles stabilized with ceftriaxone on *Escherichia coli* using atomic force microscopy. New J Chem. 38 (2014) 5633-5640

81. S. Pal, K. Mitra, S. Azmi, J.K. Ghosh, T.K. Chakraborty. Towards the synthesis of sugar amino acid containing antimicrobial noncytotoxic CAP conjugates with gold nanoparticles and a mechanistic study of cell disruption. Org Biomol Chem. 9 (2011) 4806-4810

82. A. Rai, S. Pinto, M.B. Evangelista, H. Gil, S. Kallip, M.G. Ferreira, L. Ferreira. High-density antimicrobial peptide coating with broad activity and low cytotoxicity against human cells. Acta Biomater. 33 (2016) 64-77

83. A. Rai, S. Pinto, T.R. Velho, A.F. Ferreira, C. Moita, U. Trivedi, M. Evangelista, M. Comune, K.P. Rumbaugh, P.N. Simoes, L. Moita, L. Ferreira. One-step synthesis of high-density peptide-conjugated gold nanoparticles with antimicrobial efficacy in a systemic infection model. Biomaterials. 85 (2016) 99-110

84. Z.V. Feng, T.A. Qiu, K.R. Hurley, L.H. Nyberg, H. Frew, K.P. Johnson, A.M. Vartanian, L.M.Jacob, S.E. Lohse, M.D. Torelli, R.J. Hamers, C.J. Murphy, C.L. Haynes.Impacts of gold nanoparticle charge and ligand type on surface binding and toxicity to Gram-negative and Gram-positive bacteria. Chem Sci. 6 (2015) 5186-5196

85. X. Li,S.M. Robinson, A. Gupta, K. Saha, Z. Jiang, D.F. Moyano, A. Sahar, M.A. Riley,V.M. Rotello. Functional gold nanoparticles as potent antimicrobial agents against multi-drug-resistant bacteria. ACS Nano. 8 (2014) 10682-10686

86. S.C. Hayden, G. Zhao, K. Saha, R.L. Phillips, X. Li,O.R. Miranda, V.M. Rotello, M.A. El-Sayed, I. Schmidt-Krey, U.H. Bunz. Aggregation and interaction of cationic nanoparticles on bacterial surfaces. J Am Chem Soc. 134 (2012) 6920-6923

87. K. Greish, G. Thiagarajan, H. Herd, R. Price, H. Bauer, D. Hubbard, A. Burckle, S. Sadekar, T. Yu, A. Anwar, A. Rayet, H. Ghandehari. Size and surface charge significantly influence the toxicity of silica and dendritic nanoparticles. Nanotoxicology. 6 (2012) 713-723

88. S. Gupta, R. Bansal, N. Jindal, A. Jindal. Nanocarriers and nanoparticles for skin care and dermatological treatments. Indian Dermatol Online J. 4 (2013) 267-272

89. L.A. DeLouise. Applications of nanotechnology in dermatology. J Invest Dermatol. 132 (2012) 964-975

90. S.S. Kolar, V. Luca, H. Baidouri, G. Mannino, A.M. McDermott, M.L. Mangoni. Esculentin-1a(1-21)NH: a frog skin-derived peptide for microbial keratitis. Cell Mol Life Sci.72 (2015) 617-627.

91. L. Marcellini, M. Borro, G. Gentile, A.C. Rinaldi, L. Stella, P. Aimola, D. Barra, M.L. Mangoni. Esculentin-1b(1-18)--a membrane-active antimicrobial peptide that synergizes with antibiotics and modifies the expression level of a limited number of proteins in *Escherichia coli*. FEBS J. 276 (2009) 5647-5664

92. V.P. Zharov, K.E. Mercer, E.N. Galitovskaya, M.S. Smeltzer. Photothermal nanotherapeutics and nanodiagnostics for selective killing of bacteria targeted with gold nanoparticles. Biophys J. 90 (2006) 619-627

Table 1. Comparison between molar concentration of AuNPs@Esc(1-21) and the corresponding molar concentration of Esc(1-21).

Molar concentration of AuNPs@Esc(1-21)	**Molar concentration of peptide coated onto AuNPs**
20 nM	0.35 μM
10 nM	0.17 μM
5 nM	0.08 μM

Table 2 Antimicrobial activity of Esc(1-21) and AuNPs@Esc(1-21) on both free living and biofilm forms of *P. aeruginosa* ATCC 27853

	Antibacterial Activity	
	Planktonic form	**Biofilm form**
Compound	**MBC_{50}**	**$MBEC_{50}$**
Esc(1-21)	1 μM	3 μM[a]
AuNPs@Esc(1-21)	5 nM (=0.08 μM peptide)	10 nM (=0.17 μM peptide)

[a]This value was taken from ref.[52].

FIGURE LEGENDS

Fig. 1 TEM analysis of AuNPs. A small volume of AuNPs was dropped onto a TEM grid and after drying was imaged using a TEM Tecnai F20. A) AuNPs as synthetized. B) AuNPs@PEG. C) AuNPs@Esc(1-21). Scale bar: 20 nm.

Fig. 2 Antipseudomonal activity of Esc(1-21) (panel A) or AuNPs@Esc(1-21) (panel B). Bacterial cells (4 x 10^8 CFU/mL) were incubated with different concentrations of the peptide or AuNPs@Esc(1-21) for 20 min at 37 °C. Afterwards, aliquots were withdrawn for colony counts after overnight incubation at 37 °C. Note that the concentration of peptide coated onto 2.5 nM, 5 nM, 10 nM, 20 nM and 50 nM of AuNPs@Esc(1-21) was equal to 0.04 μM, 0.08 μM, 0.17 μM, 0.35 μM and 0.87 μM, respectively. The percentage of bacterial killing was calculated compared to the control (buffer-treated bacterial cells) and is reported on the y-axis. Dotted line indicates 50% bacterial killing. Data points are the mean of triplicate samples ± SEM of three independent experiments.

Fig. 3 Antipseudomonal activity of Esc(1-21) or AuNPs@Esc(1-21) at their MBC_{50} (1 μM and 5 nM, respectively) after treatment with trypsin (0.02 μg/mL). Bacteria (4 x 10^8 CFU/mL) were incubated with the peptide/AuNPs@Esc(1-21) pre-treated with the enzyme. After 20 min at 37 °C, aliquots were withdrawn for colony counts. The percentage of bacterial killing was calculated compared to the control (buffer-treated bacterial cells) and is reported on the y-axis. Dotted line indicates 50% bacterial killing.

No killing activity was caused by the enzyme at the concentration used or AuNPs@PEG and therefore they are not shown. Data points are the mean of triplicate samples ± SEM of three independent experiments.

Fig. 4 Kinetics of cytoplasmic membrane permeabilization of *P. aeruginosa* ATCC 27853 (4 x 10^8 CFU/ml) induced by 10 nM AuNPs@Esc(1-21) or the corresponding concentration of free Esc(1-21). Bacterial cells were incubated with 1 μM Sytox Green in NaPB. Once basal fluorescence reached a constant value, 10 nM AuNPs@Esc(1-21) or AuNPs@PEG as well as the equivalent concentration of free Esc(1-21) were added, and changes in fluorescence (λ_{exc}= 485 nm, λ_{ems} = 535 nm) were monitored for 30 min. Considering the absorbance of AuNPs@PEG as a background, measurements of samples containing AuNPs@PEG were subtracted from those containing AuNPs@Esc(1-21). Control (Ctrl) was given by buffer-treated bacteria. The ratio of each value to the initial one measured after 1 min from NPs/peptide addition is reported on the y-axis. The values represent the mean of triplicate samples from a single experiment, representative of three different experiments.

Fig. 5 SEM of *P. aeruginosa* cells after 1 min (left panels) or 8 min (right panels) treatment with AuNPs@Esc(1-21) at the MBC_{50} or with AuNPs@PEG, at the same molar concentration. Controls (Ctrl) were buffer-treated cells. Insets are magnifications of image areas indicated by the black frame. Arrows indicate cell debris.

Fig. 6 TEM micrographs of *P. aeruginosa* cells after 15 min treatment with AuNPs@Esc(1-21) at the MBC_{50} **(A)** or buffer **(B)** Black arrows indicate lysed bacterial cells. Scale bar: 200 nm

Fig. 7 Effects of AuNPs@PEG or AuNPs@Esc(1-21) on the viability of HaCaT cells after 2 h treatment. Cell viability was determined by the MTT reduction to insoluble formazan (see Materials and Methods for additional details). The percentage represents the cell viability with respect to the control. Data points are the mean of triplicate samples ± SEM of three independent experiments.

Fig. 8 Effect of AuNPs@PEG and AuNPs@Esc(1-21) on the closure of a pseudo-"wound" field produced in a monolayer of HaCaT cells, seeded in each side of an ibidi culture insert. **(A):** Cells were grown to confluence and afterwards, they were treated with 5 nM AuNPs@PEG, AuNPs@Esc(1-21) or with 0.25 μM Esc(1-21). Cells were photographed at the time of insert removal (0 h) and examined for cell migration after 3, 6 and 9 h and compared to the Ctrl. All data are the mean of three independent experiments ± SEM. The levels of statistical significance between Ctrl and treated samples are indicated as follows $*p < 0.05$, $**p < 0.01$. **(B):** Micrographs showing representative results of pseudo-"wound" closure after 6 h treatment.

Fig. 9 Cartoon representing the mode of action of AuNPs@Esc(1-21) **(A)** and AuNPs@PEG **(B)** on the bacterium *P. aeruginosa.* When in contact with microbes, AuNPs@Esc(1-21) quickly concentrate on different sites of the bacterial surface, without entering into *Pseudomonas* cells, and cause disruption of the cellular structure. In contrast, despite AuNPs@PEG form clusters in solution, they are harmless to *Pseudomonas* cells and do not aggregate on their surface.

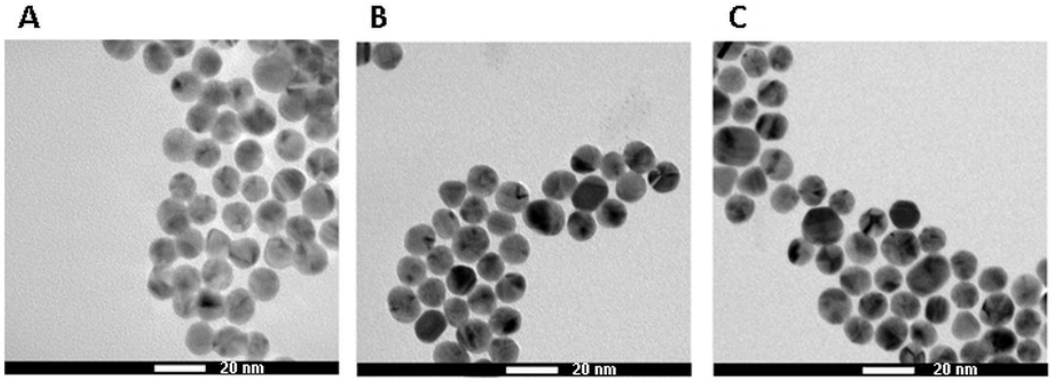

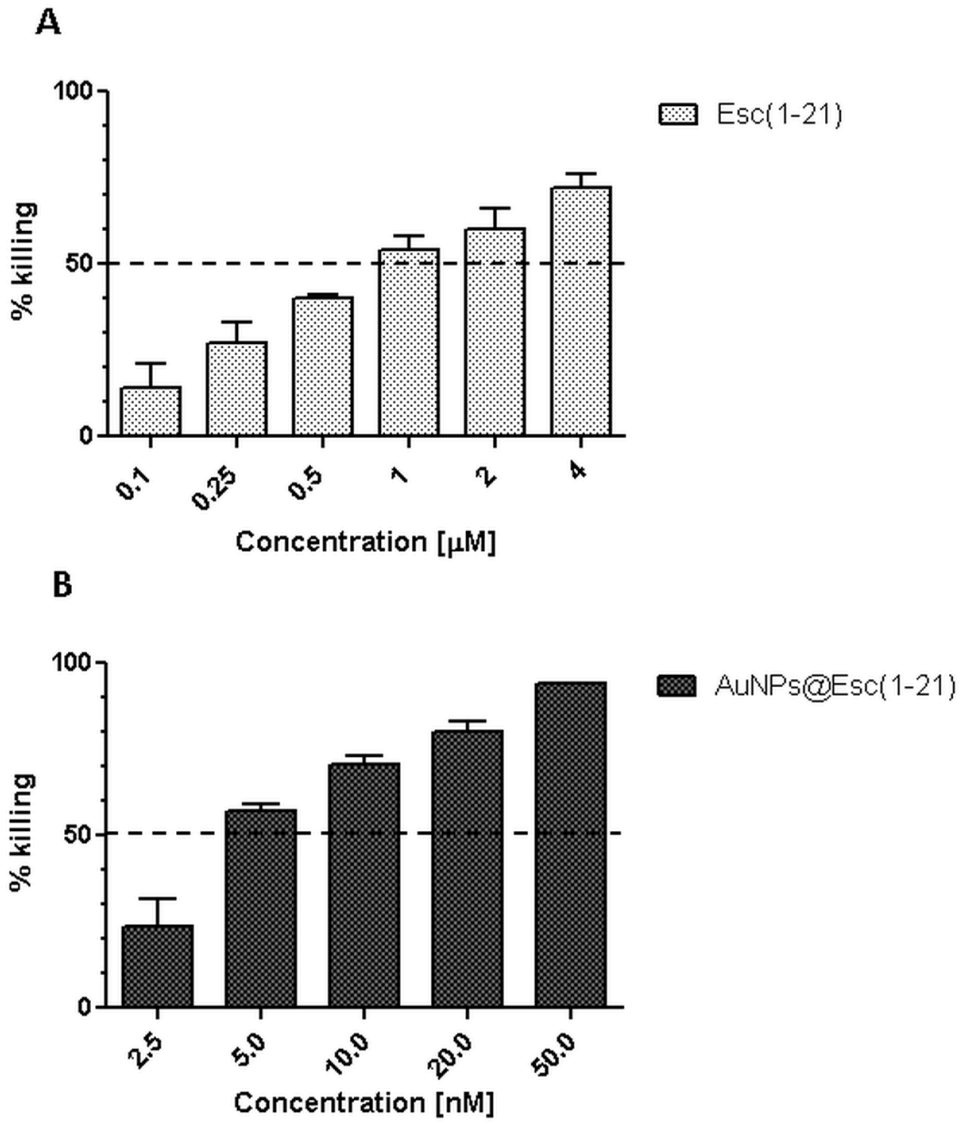

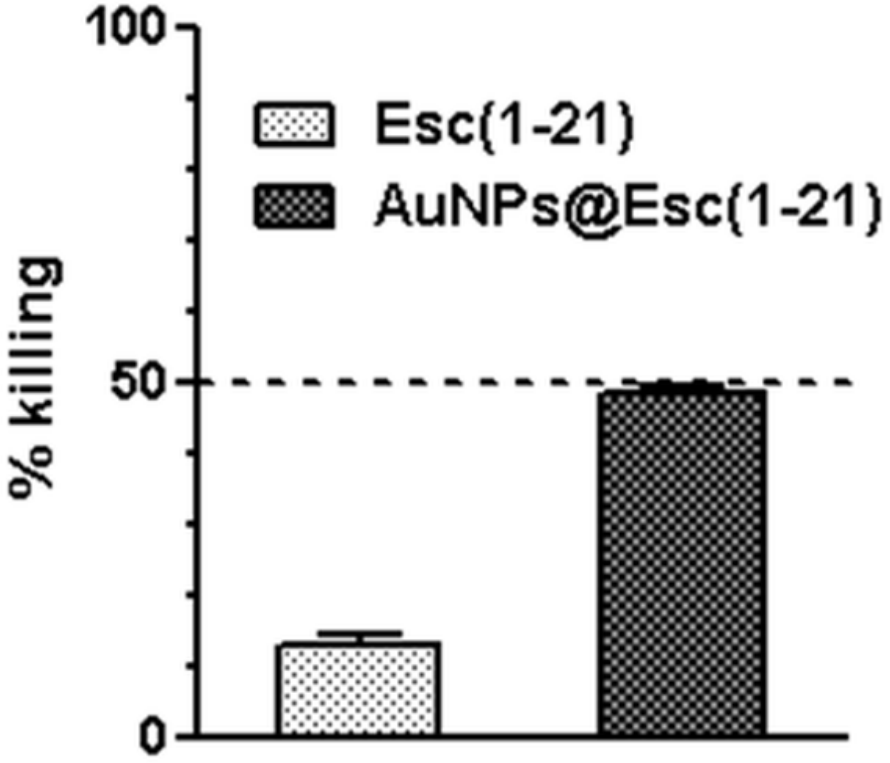

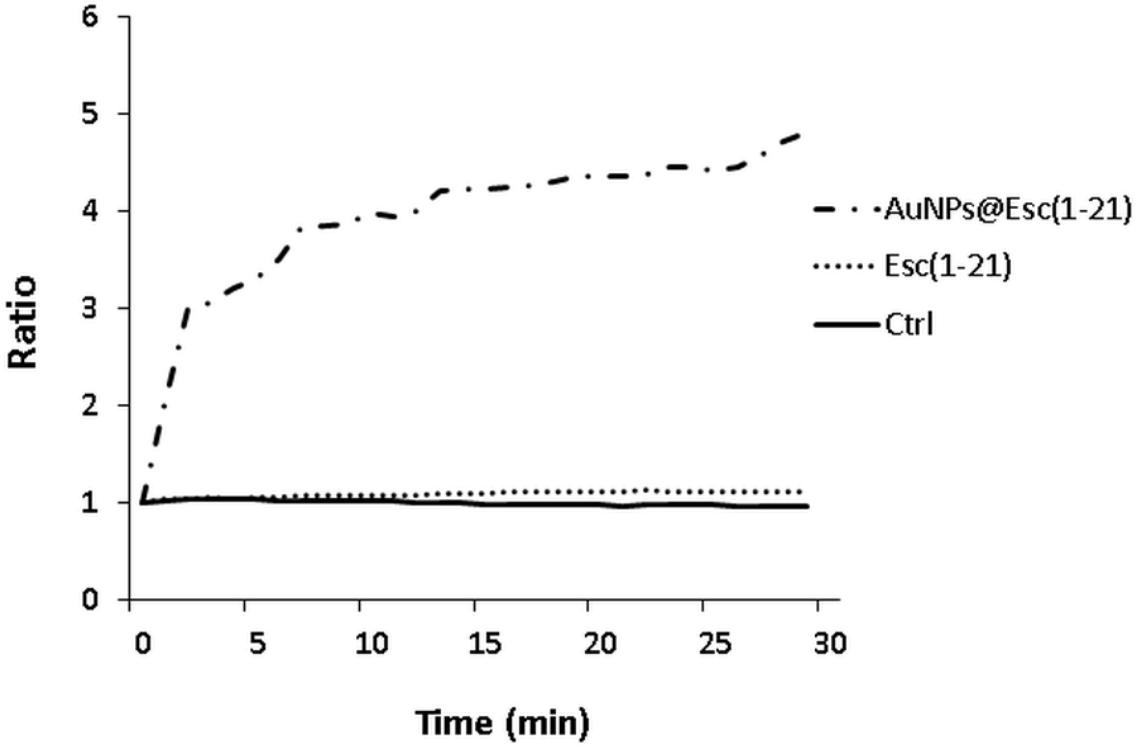

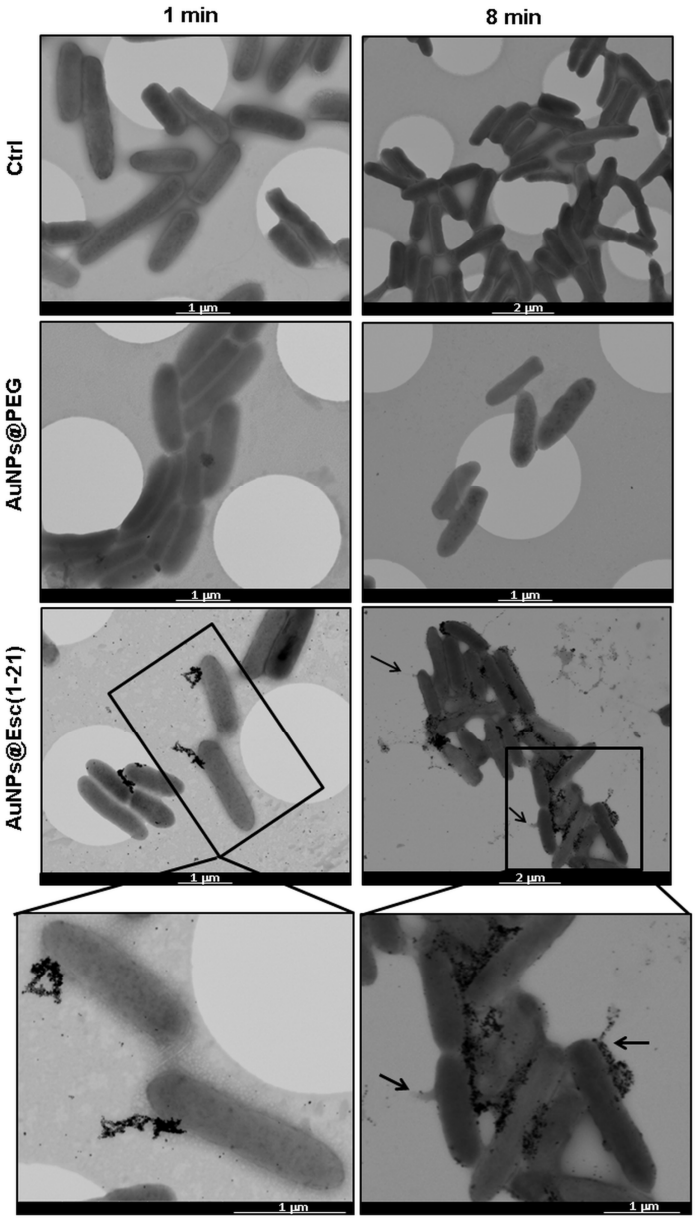

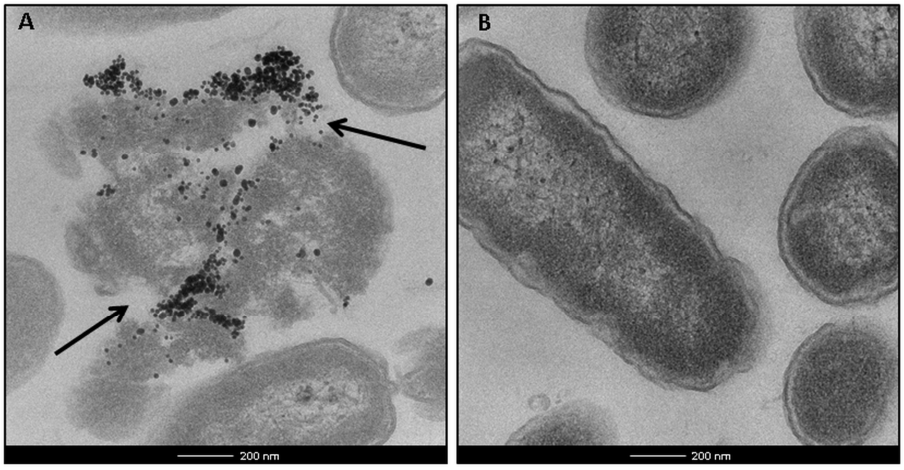

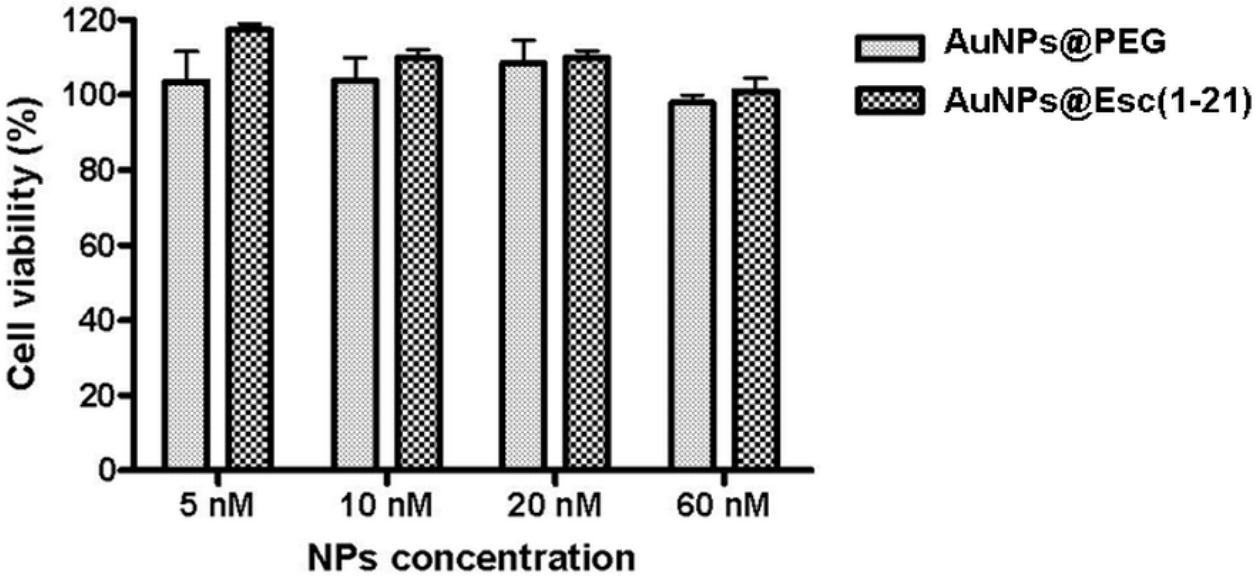

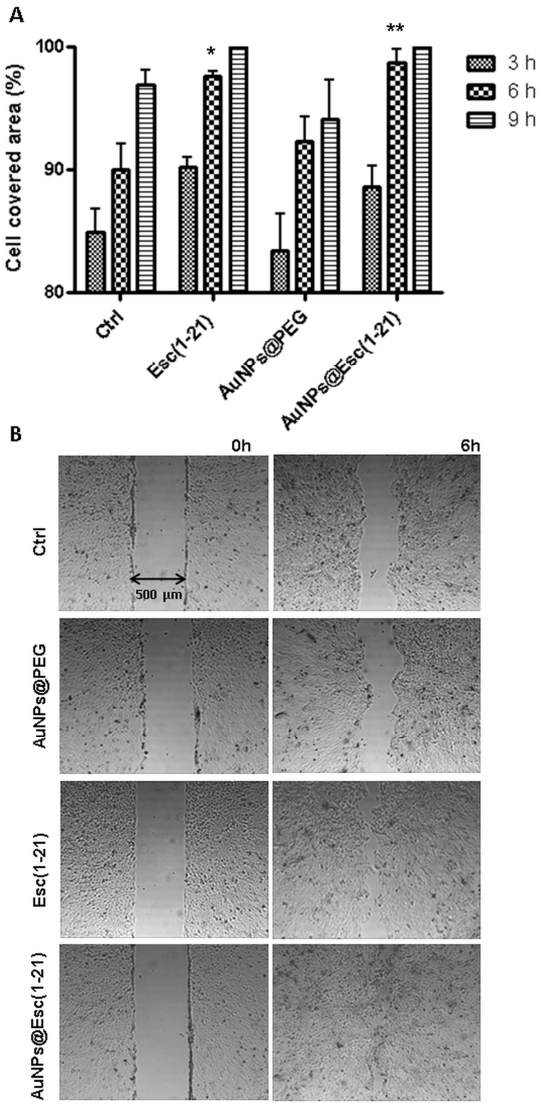

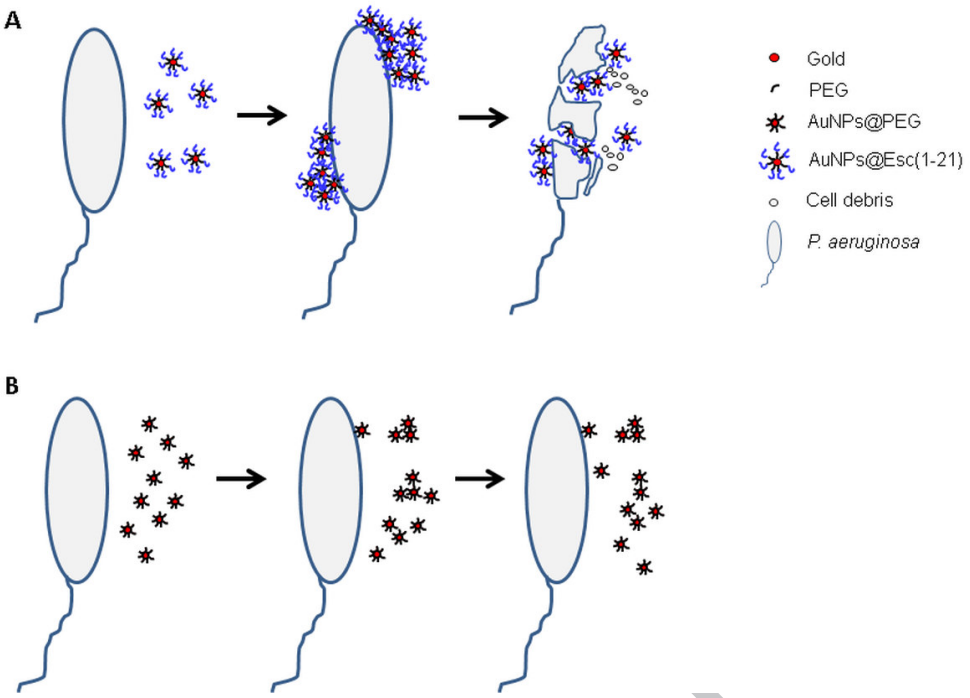

Statement of significance: Despite conjugation of AMPs to AuNPs represent a worthwhile solution to face some limitations for their development as new therapeutics, only a very limited number of studies is available on peptide-coated AuNPs. Importantly, this is the first report showing that a covalent binding of a linear AMP via a poly(ethylene glycol) linker to AuNPs highly enhances anti-*Pseudomonal* activity, preserving the same mode of action of the free peptide, without being harmful. Furthemore, AuNPs@Esc(1-21) are expected to accelerate recovery of an injured skin layer. All together, these findings suggest our peptide-coated AuNPs as attractive novel nanoscale formulation to treat bacterial infections and to heal the injured tissue.

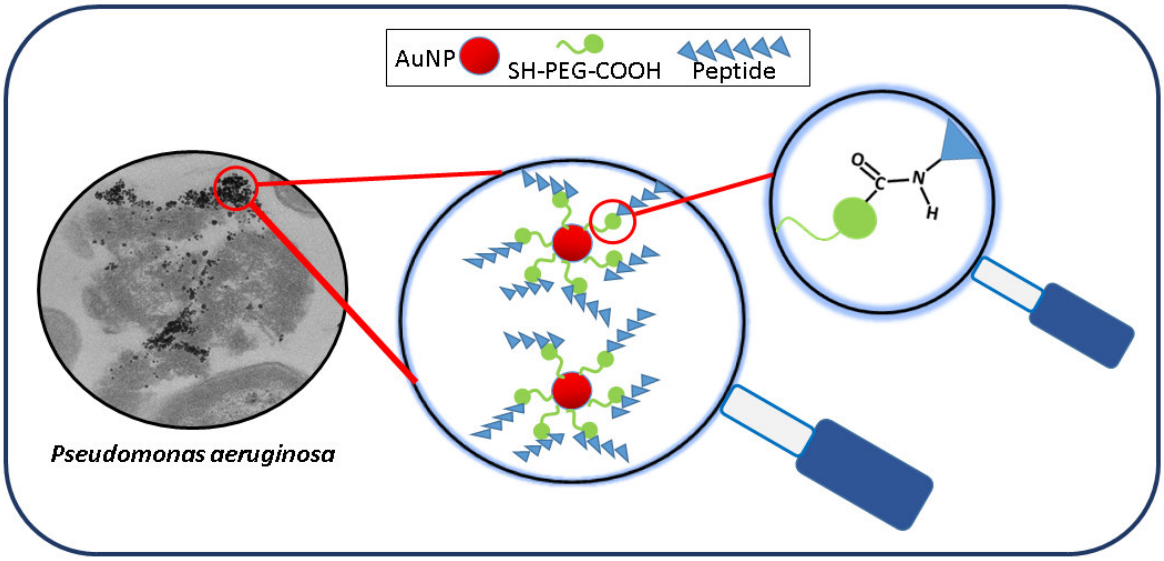

Damage of the Gram-negative bacterium *Pseudomonas aeruginosa* by Esc(1-21) peptide conjugated to gold nanoparticles (AuNPs) via PEG linker